Macromolecular Bioscience
www.mbs-journal.de

# Modification of Branched Poly(ethylene imine) with D-Fructose for Selective Delivery of siRNA into Human Breast Cancer Cells

*Jan Matthias Peschel, Liên Sabrina Reichel, Tim Hoffmann, Christoph Enzensperger, Ulrich Sigmar Schubert, Anja Traeger,* and Michael Gottschaldt**

**Branched poly(ethylene imine) (bPEI) is frequently used in RNA interference (RNAi) experiments as a cationic polymer for the delivery of small interfering RNA (siRNA) because of its ability to form stable polyplexes that facilitate siRNA uptake. However, the use of bPEI in gene delivery is limited by its cytotoxicity and a need for target specificity. In this work, bPEI is modified with D-fructose to improve biocompatibility and target breast cancer cells through the overexpressed GLUT5 transporter. Fructose-substituted bPEI (Fru—bPEI) is accessible in three steps starting from commercially available protected fructopyranosides and bPEI. Several polymers with varying molecular weights, degrees of substitution, and linker positions on D-fructose (C1 and C3) are synthesized and characterized with NMR spectroscopy, size exclusion chromatography, and elemental analysis. In vitro biological screenings show significantly reduced cytotoxicity of 10 kDa bPEI after fructose functionalization, specific uptake of siRNA polyplexes, and targeted knockdown of green fluorescent protein (GFP) in triple-negative breast cancer cells (MDA-MB-231) compared to noncancer cells (HEK293T).**

## 1. Introduction

With over 300 000 new cases and 44 000 deaths projected to occur in the USA in 2023, breast cancer represents the most common cancer and is responsible for ≈7% of all cancer-related deaths.[1] Breast cancer is categorized into different subtypes depending on the presence of molecular markers, such as hormone receptors for estrogen and progesterone or human epidermal growth factor 2 (HER2). Besides surgical removal and radiotherapy, effective treatment methods like endocrine therapy and HER2-targeted antibody therapy are available for receptor-positive subtypes, while triple-negative breast cancer is treated exclusively with chemotherapy due to the absence of the respective receptors.[2] These treatments often suffer from significant side effects due to high off-target toxicity and can be further hindered by the development of drug resistance to one or multiple chemotherapeutic agents, which results in decreased quality of life as well as much lower survival rates and high recurrence rates for triple-negative breast cancer.[3]

Gene therapy by RNA interference (RNAi) with small interfering RNA (siRNA) is a promising new addition to existing cancer therapies. siRNAs are short rigid fragments (between 15 and 30 base pairs) of natural or artificial double-stranded RNA that can induce degradation of complementary messenger RNA (mRNA) in the cytoplasm, thus preventing the translation of the corresponding gene (knockdown).[4] Over the last 25 years since its initial discovery,[5] RNAi has emerged as a powerful technique in the fight against various diseases, with several RNAi-based medications already receiving approval by the U.S. Food and Drug Administration and many more in clinical trials.[6–8]

In cancer therapy, siRNA can target key genes responsible for the development and spread of cancer. A variety of effective targets have been identified, such as growth-promoting genes (e.g., KRAS[9] and HER2[10]), anti-apoptotic genes (e.g., Bcl-2 and survivin[11,12]), mutated tumor suppressor genes (e.g., TP53[13]), and genes that induce angiogenesis (e.g., VEGF[14]). The combination of chemotherapy and simultaneous RNAi also holds great promise in helping to combat drug resistance by targeting the genes responsible for it.[15,16] For all in vivo applications, the main obstacle that any siRNA-based drug has to overcome is the delivery problem. siRNAs are vulnerable to digestion by ribonucleases and quickly get cleared from the bloodstream by renal filtration because of their small size, leading to a short serum half-life of

J. M. Peschel, L. S. Reichel, T. Hoffmann, U. S. Schubert, A. Traeger, M. Gottschaldt
Institute of Organic and Macromolecular Chemistry
Friedrich Schiller University Jena
Humboldtstrasse 10, 07743 Jena, Germany
E-mail: anja.traeger@uni-jena.de; michael.gottschaldt@uni-jena.de
C. Enzensperger
SmartDyeLivery GmbH
Botzstraße 5, 07743 Jena, Germany

The ORCID identification number(s) for the author(s) of this article can be found under https://doi.org/10.1002/mabi.202300135

© 2023 The Authors. Macromolecular Bioscience published by Wiley-VCH GmbH. This is an open access article under the terms of the Creative Commons Attribution-NonCommercial-NoDerivs License, which permits use and distribution in any medium, provided the original work is properly cited, the use is non-commercial and no modifications or adaptations are made.

**DOI: 10.1002/mabi.202300135**

around 5–60 min.[17] They are also likely to cause off-target side effects, particularly unwanted immune responses and cleavage of imperfectly matched nontarget mRNA.[18]

These challenges can be overcome through siRNA modifications or the use of delivery systems to stabilize siRNA against serum nucleases, reduce rapid renal clearance, and facilitate selective uptake into cancer cells.[19] Delivery vehicles are broadly categorized into viral and nonviral vectors. While vectors based on modified viruses can have excellent transduction efficiency, there are safety concerns regarding immunogenicity and other side effects. This has led to an increased focus on developing suitable nonviral vectors, such as lipid-based nanoparticles (LNPs), cationic polymers, and inorganic nanoparticles.[19,20] Poly(ethylene imine) (PEI) is known to be an effective and widely used cationic polymer for gene transfer applications. As such, it is a suitable platform for studies to investigate the structure–property relationships that determine the efficacy and safety of gene transfer. PEI is particularly attractive for large-scale applications due to its low cost and ease of modification, paired with favorable electronic properties. Its high positive charge density allows PEI to form stable polyplexes with genetic material to protect it from degradation. PEI also facilitates cellular uptake by interacting with negatively charged structures on cell membranes, such as heparan sulfate proteoglycans, to promote endocytosis and by inducing endosomal release through osmosis once inside the cancer cell ("proton-sponge effect").[21–23] Higher molecular weight PEI is more effective at binding genetic material, but limited by increased cytotoxicity.[24] PEI polyplexes also lack features that enable selective uptake into cancer cells.

Modification of PEI can reduce its toxicity and increase its stability in serum by shielding and diluting positive charges, for example, through PEGylation[25] or substitution with simple hydrophobic[26] or anionic groups.[27] In order to also achieve specific uptake of polyplexes into cancer cells, PEI can be modified with appropriate targeting ligands, such as antibodies,[10] folate,[28] transferrin,[29] or carbohydrates like hyaluronic acid[30] or chitosan.[31] The use of carbohydrates as targeting ligands in glycopolymer nanoparticles has been extensively studied, as their role in cellular communication and metabolism provides ample targets in receptor and transport proteins.[32] Notably, the fructose transporter protein GLUT5 has been shown to be overexpressed in breast cancer cells, including triple-negative breast cancer.[33–35] Various D-fructose-substituted nanoparticles have been synthesized to facilitate selective delivery into breast cancer tissue, such as micelles,[36] nanodiamonds,[37] carbon nanotubes,[38] and polyplexes.[39]

We previously reported the modification of linear PEI (LPEI) with D-fructose through a thiol–ene click reaction. The resulting polymers demonstrated reduced cytotoxicity in non-cancer cell lines (mouse fibroblast cells (L929) and human umbilical vein endothelial cells (HUVEC)) and targeted specific uptake of plasmid DNA (pDNA) polyplexes in the triple-negative breast cancer cell line MDA-MB-231.[39] However, these polymers are not well suited for RNAi application since the stiffness and small size of siRNA lead to reduced polyplex stability. A branched polymer architecture is preferable for siRNA complexation because positively charged amine groups on side chains provide additional stabilization to the polyplex compared to LPEI.[40,41] Previous investigations of several commercially available branched PEIs (bPEIs) have identified 10 kDa bPEI at $N/P > 5$ as the most suitable for siRNA delivery.[24] In this work, we present the modification of commercial 1.8 and 10 kDa bPEIs with D-fructose through efficient functionalization via epoxide linkers to form D-fructose substituted bPEI (Fru–bPEI) glycopolymers. Fru–bPEIs with different molecular weights, degrees of substitution (DS), and linker positions on D-fructose (C1 and C3) were synthesized to identify a suitable composition that combines low cytotoxicity, stable polyplex formation, and high target specificity for GLUT5 overexpressed cells. The polymers were tested regarding biocompatibility, siRNA polyplex stability, siRNA uptake and green fluorescent protein (GFP) knockdown specificity for breast cancer cells (MDA-MB-231, MCF-7) in comparison to noncancer cell lines (HEK293T). To the best of our knowledge, this study represents the first use of fructose-functionalized polyplexes for the selective delivery of siRNA to GLUT5 overexpressing cells.

## 2. Experimental Section

### 2.1. Materials

Branched poly(ethylene imine)s with an average molecular weight ($M_w$) of 1.8 and 10 kDa (**1.8bPEI** and **10bPEI**) were purchased from Polysciences. 2,3:4,5-Di-*O*-isopropylidene-*β*-D-fructopyranose (**iFru1–OH**) was purchased from Biosynth. Trifluoroacetic acid (TFA) was purchased from TCI. D-Fructose, racemic epichlorohydrin, and tetrabutylammonium iodide (TBAI) were purchased from Sigma–Aldrich. Dry solvents were purchased from Acros Organics. Other solvents, salts, and dialysis membranes were purchased from Carl Roth. Solvents used in chromatography were distilled prior to use. All other reagents were used without further purification. Phosphate buffered saline (PBS-1X) was prepared according to a recipe by AAT Bioquest.[42] Concentrated buffer PBS-10X was prepared similarly, but ten times more of each salt were used for the same buffer volume.

For biological investigations all the following materials were ordered from the suppliers stated in brackets: TC-treated cell culture flasks (Greiner Bio-One International GmbH, and Labsolute, Th. Geyer GmbH & Co. KG), TC-treated multiwell cell culture plates (VWR International GmbH), black 96-well plates (Nunc, Thermo Fisher), L929 cells (CLS Cell Lines Service GmbH) HEK293T cells, MCF-7 cells, and MDA-MB-231 cells (Leibniz Institute DSMZ), HEK293-GFP (Amsbio), MDA-MB-231-GFP cells (BioCat), Puromycin, Blasticidin (InvivoGen), Dulbecco's modified eagle medium (DMEM), and 4-(2-hydroxyethyl)−1-piperazineethanesulfonic acid) (HEPES) buffer 1 M (Biowest SAS), RNase-free HEPES buffer 1 M (FisherBioReagens), fetal bovine serum (FBS, Capricorn Scientific), penicillin–streptomycin, Ultra-Pure DNase/RNase-free water, trypsin supplemented with ethylenediaminetetraacetic acid (trypsin–EDTA), Quant-iT Ribogreen RNA (Invitrogen), 20% RNase-free glucose solution (Sigma–Aldrich), PrestoBlue cell viability reagent (Thermo Fisher Scientific), heparin sodium salt (Alfa Aesar), LPEI (25 kDa, Polysciences), GFP-22 siRNA and negative-control siRNA and AllStars Neg. siRNA AF488 (Qiagen). *N*-[4-(Methylsulfonyl)-2-nitrophenyl]-1,3-benzodioxol-5-amine (MSNBA), (BLDpharm), dimethylsulfoxide (DMSO, Sigma–Aldrich).


© 2023 The Authors. Macromolecular Bioscience published by Wiley-VCH GmbH

### 2.2. General Methods and Instrumentation

Reaction progress during the synthesis of D-fructose precursors was monitored by thin-layer chromatography (TLC) on glass plates coated with silica gel 60 (Merck). TLC plates were stained with 10% sulfuric acid in methanol. Polymer reactions were monitored by proton nuclear magnetic resonance ($^1$H-NMR) spectroscopy.

Chromatographic separations were performed on a Teledyne Isco CombiFlash Rf flash chromatography system using normal-phase RediSep Rf silver silica gel cartridges. NMR spectra were recorded on Bruker Avance (300, 400 MHz) or Bruker Avance Neo (500 MHz) spectrometers at room temperature. Chemical shifts ($\delta$) are expressed in parts per million relative to tetramethylsilane (TMS). NMR spectra were processed in the ACD Spectrus processor by applying automatic phase correction and matching the chemical shift of the solvent peak to a reference value. High-resolution electrospray ionization mass spectrometry (HR-ESI-MS) was performed on a Bruker MicrOTOF-QII mass spectrometer. Elemental analyses were measured on a Eurovector EA3000. Size exclusion chromatography (SEC) was performed on a Jasco LC-4000 series gel permeation chromatography system equipped with an AS-1555 autosampler, a PU-980 isocratic pump, an RI-930 refractive index detector, and a PSS NOVEMA-MAX 30 Å (5 µm) and two PSS-NOVEMA-MAX 1000 Å (5 µm) columns placed in series. 0.1% TFA in 0.1 M aqueous NaCl was used as eluent at 1 mL min$^{-1}$ flow rate and a temperature of 30 °C. Molar masses were calculated using poly(2-vinylpyridine) standards.

Dynamic light scattering (DLS) was measured with Zetasizer Ultra from Malvern Instruments. Samples were measured in disposable UV-Cuvette micro consisting of polystyrene, BRAND GmbH.

Particle uptake and knockdown studies were measured with CytoFlex Beckmann Coulter, Brea, CA, USA, PrestoBlue assay, RiboGreen binding assay, and heparin dissociation assay were measured with the multiplate reader Tecan infinite M200Pro, Germany.

#### *2.2.1. Synthesis of 1,2:4,5-Di-O-Isopropylidene-β-D-Fructopyranoside (**iFru3—OH**)*

The synthesis was performed according to a literature procedure.[43] Briefly, D-fructose (36 g, 200 mmol) was suspended in dry acetone (700 mL). Concentrated sulfuric acid (3 mL) was added, and the solution was stirred at room temperature for 90 min, after which most of the sugar had dissolved. The reaction was quenched with 2.75 M NaOH (100 mL). Acetone was removed in vacuo; water (50 mL) was added; and the mixture was extracted with dichloromethane (DCM, 3 × 150 mL). The combined organic phases were washed twice with brine (70 mL), dried over $Na_2SO_4$, and the solvent was removed in vacuo. The residue (32 g) was dissolved in boiling diethyl ether (200 mL), and *n*-pentane (120 mL) and diethyl ether (30 mL) were added. Upon cooling to 8 °C, **iFru3—OH** crystallized as white needles, which were washed thrice with *n*-pentane (50 mL) and dried in vacuo. Yield: 17.39 g (33%).

mp: 119.5 °C. $^1$H-NMR (300 MHz, $CDCl_3$, $\delta$): 4.23 (dd, $J_1$ = 5.9 Hz, $J_2$ = 2.1 Hz, 1H, H5), 4.20 (d, $J$ = 8.9 Hz, 1H, H1), 4.16 (m, 1H, H4), 4.12 (m, 1H, H6), 4.02 (d, $J$ = 13.3 Hz, 1H, H6′), 4.00 (d, $J$ = 8.9 Hz, 1H, H1′), 3.68 (t, $J$ = 7.5 Hz, 1H, H3), 2.03 (d, $J$ = 8.2 Hz, 1H, OH), 1.55 + 1.53 + 1.46 + 1.39 (4s, 12H, $CH_3$).

#### *2.2.2. Synthesis of 1-O-Glycidyl-2,3:4,5-di-O-Isopropylidene-β-D-Fructopyranoside (**iFru1—GE**)*

**iFru1—GE** was prepared by an adapted literature procedure.[44] **iFru1—OH** (5.0 g, 19.2 mmol) and TBAI (1.70 g, 4.6 mmol) were dissolved in tetrahydrofuran (THF, 20 mL). Saturated aqueous NaOH (30 mL) was added, and the solution was stirred for 5 min. Epichlorohydrin (4.0 mL, 51 mmol) was added, and the mixture was heated to 50 °C under vigorous stirring. After 48 h, TLC indicated complete conversion of the educt (1:1 *n*-heptane/ethyl acetate, $R_f$ = 0.62). Brine (100 mL) and water (100 mL) were added, and the aqueous layer was extracted with DCM (3 × 150 mL). The combined organic phases were dried over $Na_2SO_4$, and the solvent was removed in vacuo. 6:1 *n*-pentane/ethyl acetate (50 mL) was added, forming a white precipitate, which was filtered off and washed with *n*-pentane/ethyl acetate (2 × 50 mL). The filtrate was dried in vacuo (6.76 g pale yellow oil).

The crude product was purified via flash chromatography using a 120 g cartridge at a flow rate of 85 mL min$^{-1}$ with a gradient of ethyl acetate in *n*-heptane as eluent (25–50% vol) to give the glycidyl ether **iFru1—GE** as a colorless oil. Yield: 4.88 g (80%).

$^1$H-NMR (500 MHz, $CDCl_3$, $\delta$): 4.61 (dd, $J_1$ = 7.9 Hz, $J_2$ = 2.6 Hz, 1H, H4), 4.41 (d, $J$ = 2.6 Hz, 0.5H, H3b), 4.39 (d, $J$ = 2.6 Hz, 0.5H, H3a), 4.24 (dd, $J_1$ = 7.9 Hz, $J_2$ = 1.2 Hz, 1H, H5), 3.92 (dd, $J_1$ = 1.8 Hz, $J_2$ = 12.9 Hz, 1H, H6), 3.89 (dd, $J_1$ = 11.6 Hz, $J_2$ = 3.1 Hz, 0.5H, H7b), 3.78 (dd, $J_1$ = 11.6 Hz, $J_2$ = 3.1 Hz, 0.5H, H7a), 3.74 (d, $J$ = 12.9 Hz, 1H, H6′), 3.66 (2d, $J$ = 10.8 Hz, 1H, H1), 3.63 (2d, $J$ = 10.8 Hz, 1H, H1′), 3.61 (dd, $J_1$ = 11.6 Hz, $J_2$ = 5.5 Hz, 0.5H, H7′a), 3.45 (dd, $J_1$ = 11.5 Hz, $J_2$ = 6.1 Hz, 0.5H, H7′b), 3.16 (m, 1H, H8), 2.79 (2dd, $J_1$ = 5.0 Hz, $J_2$ = 1.2 Hz, 1H, H9), 2.64 (dd, $J_1$ = 5.0 Hz, $J_2$ = 2.7 Hz, 0.5H, H9′a), 2.61 (dd, $J_1$ = 5.0 Hz, $J_2$ = 2.8 Hz, 0.5H, H9′b), 1.55 (2s, 3H, H12), 1.48–1.47 (2s, 3H, H14), 1.45–1.44 (2s, 3H, H11), 1.35 (s, 3H, H15); $^{13}$C-NMR (125 MHz, $CDCl_3$, $\delta$): 108.92 (C13), 108.60 + 108.58 (C10), 102.53 (C2), 72.84 (C7b), 72.64 (C1), 72.36 (C7a), 70.97 (C5), 70.15 (C4), 70.04 (C3), 61.02 (C6), 50.69 (C8b), 50.55 (C8a), 44.27 + 44.18 (C9), 26.54 (C12), 25.85 (C14), 25.26 + 25.24 (C11), 24.01 (C15); HR-ESI-MS $m/z$: $[M + Na]^+$ calcd. for $C_{15}H_{24}O_7$, 339.1414; found, 339.1423. Anal. Calcd. for $C_{15}H_{24}O_7$: C 56.95, H 7.65; found: C 56.77, H 7.64.

#### *2.2.3. Synthesis of 3-O-Glycidyl-1,2:4,5-di-O-Isopropylidene-β-D-Fructopyranoside (**iFru3—GE**)*

**iFru3—GE** was prepared according to the same procedure as **iFru1—GE**, starting with D-fructopyranoside **iFru3—OH** (3.25 g, 12.5 mmol), TBAI (1.20 g, 3.2 mmol), and epichlorohydrin (2.0 mL, 25.0 mmol). **iFru3—GE** was obtained as a colorless oil. Yield: 2.68 g (68%).

$^1$H-NMR (500 MHz, $CDCl_3$, $\delta$): 4.30 + 4.29 (2t, $J$ = 5.6 Hz, 1H, H4), 4.2 (m, 1H, H5), 4.19 (dd, $J_1$ = 11.6 Hz, $J_2$ = 2.9 Hz, 0.5H, H7b), 4.19 + 4.15 (2d, $J$ = 8.5 Hz, 1H, H1), 4.12 (dd, $J_1$ = 13.4 Hz,


© 2023 The Authors. Macromolecular Bioscience published by Wiley-VCH GmbH

**Table 1.** Stoichiometry for the synthesis of iFru–bPEIs and their expected and found primary degree of substitution. Samples are named according to the template iFru*X*(*Y*)-*Z*bPEI, where iFru is isopropylidene-protected D-fructose, *X* is the linker position on D-fructose moieties, *Y* is the pDS rounded to the nearest 5%, and *Z* is the $M_w$ of the educt bPEI in kDa.

| | iFru-GE | | bPEI | | $V_{MeOH}$ [mL] | Yield [mg] | pDS [%] | |
|---|---|---|---|---|---|---|---|---|
| | *m* [mg] | $n_{fru}$ [mmol] | *m* [mg] | $n_{bPEI}$ [mmol] | | | Calcd. | Found |
| **iFru1(80)–1.8bPEI** | 880 | 2.78 | 500 | 11.6 | 10 | 860 | 83 | 78 |
| **iFru3(85)–1.8bPEI** | 675 | 2.13 | 388 | 9.00 | 10 | 974 | 82 | 86 |
| **iFru1(30)–10bPEI** | 194 | 0.61 | 255 | 5.93 | 10 | 419 | 33 | 28 |
| **iFru1(55)–10bPEI** | 2052 | 6.49 | 1424 | 33.1 | 20 | 2900 | 61 | 55 |
| **iFru1(80)–10bPEI** | 2030 | 6.42 | 1036 | 24.1 | 16 | 2803 | 85 | 82 |
| **iFru1(110)–10bPEI** | 343 | 1.09 | 107 | 2.48 | 10 | 331 | 137 | 108 |
| **iFru1(190)–10bPEI** | 454 | 1.44 | 61 | 1.43 | 9 | 267 | 321 | 191 |
| **iFru3(80)–10bPEI** | 699 | 2.21 | 391 | 9.07 | 10 | 935 | 78 | 78 |

$J_2$ = 2.6 Hz, 1H, H6) 4.00 (dd, $J_1$ = 13.4 Hz, $J_2$ = 2.5 Hz, 1H, H6′), 3.98 (dd, $J_1$ = 11.6 Hz, $J_2$ = 4.6 Hz, 0.5H, H7a) 3.98 + 3.95 (2d, $J$ = 8.5 Hz, 1H, H1′), 3.81 (dd, $J_1$ = 11.6 Hz, $J_2$ = 3.0 Hz, 0.5H, H7′a), 3.5 (d, $J$ = 7.4 Hz, 0.5H, 3b), 3.49 (dd, $J_1$ = 11.5 Hz, $J_2$ = 6.5 Hz, 0.5H, H7′b), 3.42 (d, $J$ = 7.3 Hz, 0.5H, 3a), 3.21–3.17 (m, 0.5H, 8b), 3.17–3.13 (m, 0.5H, 8a), 2.79 (2t, $J$ = 5 Hz, 1H, H9), 2.72 (dd, $J_1$ = 5.1 Hz, $J_2$ = 2.7 Hz, 0.5H, H9′a), 2.59 (dd, $J_1$ = 4.9 Hz, $J_2$ = 2.7 Hz, 0.5H, H9′b), 1.55 + 1.54 (2s, 3H, H14), 1.51 + 1.50 (2s, 3H, H12), 1.43 + 1.41 (2s, 3H, H11), 1.37 + 1.36 (2s, 3H, H15); $^{13}$C-NMR (125 MHz, $CDCl_3$, $\delta$): 112.23 + 112.18 (C10), 109.08 + 109.05 (C13), 104.33 + 104.27 (C2), 77.74 (C3a), 77.54 + 77.40 (C4), 77.35 (C3b), 73.84 + 73.78 (C5), 72.92 (C7b), 71.81 + 71.76 (C1), 71.22 (C7a), 60.18 + 60.09 (C6), 51.03 (C8b), 50.63 (C8a), 44.27 + 44.19 (C9), 28.16 + 28.11 (C14), 26.92 + 26.85 (C12), 26.26 + 26.18 (C15), 25.94 + 25.91 (C11); HR-ESI-MS *m*/*z*: $[M + Na]^+$ calcd. for $C_{15}H_{24}O_7$, 339.1414; found, 339.1410. Anal. Calcd. for $C_{15}H_{24}O_7$: C 56.95, H 7.65; found: C 56.74, H 7.64.

### 2.2.4. Fructosylation of bPEI

*Synthesis of **iFru1(80)–1.8bPEI***: **1.8bPEI** and **iFru1–GE** were dissolved in MeOH (10 mL) in a sealed vial and stirred at 40–50 °C for 3 days. The resulting solution was dialyzed against 15% MeOH in water using a Biotech CE membrane with a molecular weight cutoff (MWCO) of 100–500 Da. The dialysate was exchanged once after 5 h. After 24 h, the polymer solution was removed, and the tubing was rinsed with MeOH. MeOH was removed in vacuo, followed by lyophilization to yield **iFru1(80)–1.8bPEI** as a white solid.

*Synthesis of **iFru3(85)–1.8bPEI***: **iFru3(85)–1.8bPEI** was prepared according to the same procedure. **iFru3–GE** was used instead of **iFru1–GE**.

*Synthesis of **iFru1(30/55/80/110/190)–10bPEI***: **10bPEI** and **iFru1–GE** were dissolved in MeOH in a sealed vial and stirred at 40–50 °C for 10 days (only 5 days for **iFru1(30)–10bPEI**, 14 days for **iFru1(190)–10bPEI**). The resulting solution was dialyzed against MeOH using a Spectra Por 7 membrane with an MWCO of 1 kDa. After 24 h, the polymer solution was removed, and the tubing was rinsed with MeOH. The products were dried in vacuo, yielding the polymers **iFru1(30/55/80/110/190)–10bPEI** as white to off-white solids.

*Synthesis of **iFru3(80)–10bPEI***: **iFru3(80)–10bPEI** was prepared according to the same procedure. **iFru3–GE** was used instead of **iFru1–GE**.

Unreacted fructose epoxide was removed after the reaction using dialysis. iFru–1.8bPEIs were dialyzed against a mix of methanol and water instead of pure methanol as this led to less product being lost in dialysis. iFru–10bPEIs were dialyzed in pure methanol because of their limited solubility in water mixtures.

**Table 1** summarizes the stoichiometry used for the synthesis. The expected primary degree of substitution (pDS) was calculated based on the formula

$$\mathrm{pDS} = 3 \cdot n_{fru} \cdot n_{bPEI}^{-1} \cdot w_{bPEI}^{-1} \quad (1)$$

in which $n_{fru}$ is the amount of fructose derivatives **iFru1–GE** or **iFru3–GE**, $n_{bPEI}$ is the amount of repeating units of bPEI, calculated using the molar mass of an individual repeating unit ($C_2H_4NH$, $M$= 43.07 g mol$^{-1}$), and $w_{bPEI}$ is the mass fraction of bPEI (to account for water content), which was determined via elemental analysis to be 0.87 for **1.8bPEI** and 0.96 for **10bPEI**.

To determine the composition of the synthesized polymers, the integral of the isopropylidene signal (12H) was compared to the integral of the bPEI backbone (4H for DS, 12H for pDS). The signal of one $CH_2$ group of the linker was overlapped with the backbone signal and thus needed to be subtracted from it, resulting in the following formula for pDS calculation

$$\mathrm{pDS} = \mathrm{AUC}_{iso} \cdot \left(\mathrm{AUC}_{bPEI} - \frac{1}{6}\mathrm{AUC}_{iso}\right)^{-1} \quad (2)$$

$AUC_{iso}$ was obtained by integrating the signals belonging to the isopropylidene protecting groups (1.8–1.2 ppm) and $AUC_{bPEI}$ was obtained by integrating the signals belonging to the polymer backbone (3.1–2.2 ppm).

*iFru1-bPEIs*: $^1$H-NMR (400 MHz, $CDCl_3$, $\delta$): 4.63 (1H, H4), 4.40 (1H, H3), 4.25 (1H, H5), 3.98–3.78 (2H, H6+H8), 3.69–3.43 (5H, H6′+H1+H7), 3.10–2.20 (H9+$CH_2$(bPEI)), 1.70–1.20 (12H, $CH_3$).


© 2023 The Authors. Macromolecular Bioscience published by Wiley-VCH GmbH

*iFru3-bPEIs*: $^{1}$H-NMR (400 MHz, $CDCl_3$, $\delta$): 4.35–4.05 (4H, H4+H5+H1+H6), 4.03–3.75 (4H, H6′+H1′+H7+H8), 3.65–3,50 (1H, H7′), 3.49–3.39 (1H, H3), 3.10–2.20 (H9+$CH_2$(bPEI)), 1.70-1.20 (12H, $CH_3$).

### 2.2.5. Deprotection of iFru–bPEIs (*Fru1(80)–1.8bPEI*, *Fru3(85)–1.8bPEI*, *Fru1(30/55/80/110/190)–10bPEI*, and *Fru3(80)–10bPEI*)

The isopropylidene-protected polymer was dissolved in a 4:1 mixture of TFA and water to a concentration of ≈0.1–0.2 g $mL^{-1}$, then stirred for 6 h at room temperature. The polymer was crashed in diethyl ether (5–10 times the volume of the reaction mixture) and centrifuged. The supernatant was discarded, and the residue was washed with diethyl ether (30 mL) and dissolved in a small amount of PBS-10X (up to two times the volume of the initial reaction mixture, depending on solubility). The solution was dialyzed using Biotech CE membranes with an MWCO of 100–500 Da for polymers produced from **1.8bPEI**. Spectra Por 7 membranes with an MWCO of 1 kDa were used for polymers produced from **10bPEI**. The dialysate was exchanged twice per day. The sample was dialyzed twice against PBS-1X, twice against 1 M NaCl (only for Cl variants), then twice against water (strong osmotic swelling). The polymer was lyophilized to obtain a white-to-yellow solid and stored at −20 °C. Yield: 147 mg **Fru1(80)–1.8bPEI–PBS**, 130 mg **Fru1(80)–1.8bPEI–Cl**, 836 mg **Fru3(85)–1.8bPEI–Cl**, 394 mg **Fru1(30)–10bPEI–PBS**, 3251 mg **Fru1(55)–10bPEI–PBS**, 1638 mg **Fru1(80)–10bPEI–PBS**, 706 mg **Fru1(80)–10bPEI–Cl**, 300 mg **Fru1(110)–10bPEI–PBS**, 185 mg **Fru1(190)–10bPEI–Cl**, and 933 mg **Fru3(80)–10bPEI–Cl**.

$^{19}$F- and $^{31}$P-NMR were used to verify the successful removal of trifluoroacetate and hydrogen phosphates (only for Cl variants). For uptake and transfection trials, 5 mg $mL^{-1}$ aqueous stock solutions of Fru–bPEIs were prepared and stored at −20 °C.

*$^{1}$H-NMR (400 MHz, $D_2O$, $\delta$)*: The attached D-fructose moieties formed a mixture of several isomers, leading to broad and overlapping signals. Fructose signals were detected in the range 4.25–3.0 ppm and signals of the bPEI backbone were located in the range 3.5–2.0 ppm.

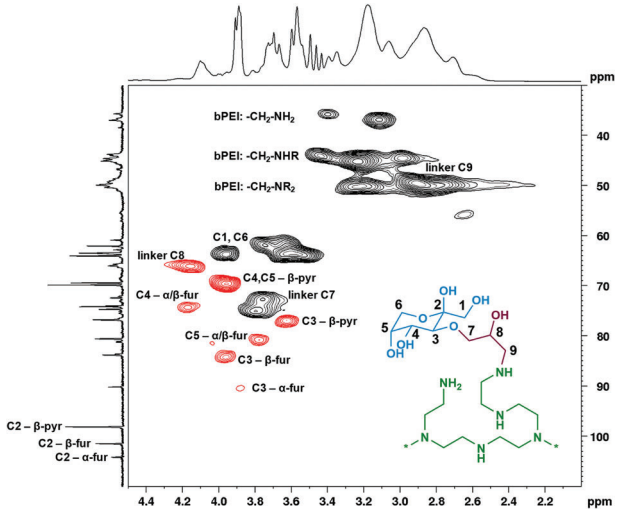


**Figure 1.** ASAP-HSQC NMR of **Fru3(85)–1.8bPEI** (400 MHz, $D_2O$). Fructose signals were assigned to their respective isomers by matching their shifts to reference data for D-fructose.[50] C3 is shifted downfield by the adjacent ether group.

Assigned HSQC-Spectra of Fru–1.8bPEIs are further presented in **Figure 1** and Figure S13 (Supporting Information).

**Table 2** summarizes the yields of Fru–bPEIs as well as the results of elemental analysis. Expected CHN content for elemental analysis was calculated from the sum formula $(C_2H_4NH)_3(C_9H_{16}O_7)_{pDS}$ using the found pDS obtained by $^{1}$H-NMR-analysis of iFru–bPEIs as input. The polymer content (weight fraction $w$) of Fru–bPEIs was calculated by dividing the found nitrogen content by the expected nitrogen content.

### 2.2.6. Cell Culture

L929 (mouse fibroblast cell line), HEK293T (human embryonic kidney cell line), MDA-MB-231 (triple-negative human breast adenocarcinoma cell line), MCF-7 (estrogene, progesterone, and glucocorticoid receptor positive human breast adenocarcinoma cell line), and HEK293-GFP (human embryonic kidney cell line labeled with GFP), MDA-MB-231-GFP (triple-negative human

**Table 2.** Elemental analysis of Fru–bPEIs.

| Name | Anion | Anal. Calcd. [%] | | | Anal. Found [%] | | | | $w$ [%] |
|---|---|---|---|---|---|---|---|---|---|
| | | C | H | N | C | H | N | Cl | |
| **Fru1(80)–1.8bPEI** | PBS | 49.89 | 8.84 | 13.41 | 39.45 | 8.00 | 11.03 | 13.37 | 82 |
| | Cl | 49.89 | 8.84 | 13.41 | 35.32 | 7.41 | 9.91 | 17.89 | 74 |
| **Fru3(85)–1.8bPEI** | Cl | 49.64 | 8.71 | 12.59 | 33.02 | 6.87 | 8.92 | 22.49 | 71 |
| **Fru1(30)–10bPEI** | PBS | 52.39 | 10.06 | 21.54 | 34.65 | 8.14 | 14.08 | 3.86 | 66 |
| **Fru1(55)–10bPEI** | PBS | 50.74 | 9.25 | 16.17 | 35.06 | 8.00 | 11.44 | 9.25 | 71 |
| **Fru1(80)–10bPEI** | PBS | 49.75 | 8.77 | 12.97 | 37.15 | 8.03 | 10.09 | 3.86 | 78 |
| | Cl | 49.75 | 8.77 | 12.97 | 40.32 | 8.24 | 10.91 | 13.02 | 84 |
| **Fru1(110)–10bPEI** | PBS | 49.12 | 8.46 | 10.91 | 40.80 | 8.00 | 9.31 | 2.15 | 85 |
| **Fru1(190)–10bPEI** | Cl | 47.99 | 7.91 | 7.23 | 44.02 | 7.77 | 6.79 | 5.55 | 94 |
| **Fru3(80)–10bPEI** | Cl | 49.93 | 8.86 | 13.54 | 37.74 | 8.13 | 10.69 | 15.43 | 79 |


© 2023 The Authors. Macromolecular Bioscience published by Wiley-VCH GmbH

breast adenocarcinoma cell line labeled with enhanced green fluorescent protein (eGFP)) were cultured in DMEM (1 g $L^{-1}$ glucose, supplemented with 10% (v/v) FBS, 100 U $mL^{-1}$ penicillin, 100 µg $mL^{-1}$ streptomycin) (D10). For selectively cultivated GFP-labeled, puromycin-resistant MDA-MB-231-GFP cells and blasticidin-resistant HEK293-GFP cells, puromycin at a final concentration of 1 µg $mL^{-1}$ and blasticidin at a concentration of 10 µg $mL^{-1}$ was added to the MDA-MB-231-GFP and HEK293-GFP cell line. All cell lines were cultivated at 37 °C in a humidified 5% (v/v) $CO_2$ incubator. One day before the experiment, for cytotoxicity assay L929 cell line was seeded in a 96-well plate at $0.1 \times 10^6$ cells $mL^{-1}$ in 100 µL D10. For particle uptake and knockdown studies, HEK293T or HEK293-GFP was seeded in a 24-well plate at $0.2 \times 10^6$ cells $mL^{-1}$ in 500 µL D10 supplemented with 10 mM HEPES (D10H). MDA-MB-231, MCF-7, and MDA-MB-231-GFP were seeded in a 24-well plate at $0.3 \times 10^6$ cells $mL^{-1}$ in 500 µL D10 supplemented with 10 mM HEPES (D10H). Cells were preincubated for 24 h for attaching to the well surface. One hour before the experiment started, the medium was changed to 450 µL fresh D10H.

#### 2.2.7. Cytotoxicity Study

To determine the biocompatibility of the polymer with different degrees of D-fructose substitution, PrestoBlue assay was performed in L929 cells (based on ISO10993-5) over 24 h. For this purpose, L929 was seeded in a 96-well plate one day before treatment to ensure cell attachment. The outer wells were excluded. After 24 h of preincubation, the old medium was replaced by 100 µL of a solution containing the polymers dissolved and diluted in D10 at the targeted concentration. 24 h later, the medium was replaced by a 10% (v/v) PrestoBlue solution in fresh culture medium, prepared according to the manufacturer's instructions. The cells were further incubated for 45 min before fluorescence was measured at $\lambda_{Ex} = 570/\lambda_{Em} = 610$ nm. Nontreated control cells were referred to as 100% viability, and values lower than 70% were regarded as cytotoxic. The relative percentage of viable cells was calculated as follows

$$\text{Viability}/\% = \frac{FI_{Sample} - FI_0}{FI_{Ctrl} - FI_0} \times 100 \quad (3)$$

$FI_{Sample}$, $FI_0$, and $FI_{Ctrl}$ represent the fluorescence intensity of a given sample, medium without cells (the blank), and nontreated control (100% viability), respectively.

#### 2.2.8. RiboGreen Binding Assay and Heparin Dissociation Assay

siRNA–polymer interaction was investigated with RiboGreen binding assay followed by a heparin dissociation assay. The assay was based on the increased fluorescence intensity of RiboGreen when intercalating with the genetic material and decreased fluorescence intensity when RiboGreen is not intercalating.

First, the master mix of diluted genetic material and RiboGreen was prepared. In detail, 15 µg $mL^{-1}$ negative-control siRNA and RiboGreen were diluted in RNase-free HBG buffer (20 mM HEPES and 5% (w/v) glucose) and incubated in the dark for 10 min at room temperature. The polymers were diluted in a black 96-well plate with RNase-free HBG buffer to give N/P ratios ranging from 1 to 30. An equal volume of the master mix was added to the polymer solutions, mixed by resuspension, and incubated at 37 °C for 15 min. The fluorescence intensity was measured at $\lambda_{Ex} = 525$ nm/$\lambda_{Em} = 605$ nm. The sample containing genetic material and RiboGreen was the 100% control.

Heparin dissociation assay was performed subsequently to the RiboGreen binding assay. Heparin was added automatically to the polyplex–RiboGreen mixtures by the dispenser of the multiplate reader to obtain the targeted concentrations (Table S1, Supporting Information). After each addition, the plate was shaken and incubated at 37 °C for 10 min, then fluorescence intensity was measured. The percentage of displaced RiboGreen due to polyplex formation or re-intercalating following siRNA release by heparin was calculated as follows

$$\text{rFI}/\% = \frac{FI_{Sample}}{FI_{siRNA}} \times 100 \quad (4)$$

rFI is the relative fluorescence intensity and $FI_{Sample}$, and $FI_{siRNA}$ is the fluorescence intensities of the sample and the RiboGreen intercalated into genetic material (100%).

#### 2.2.9. Time-Dependent Investigation of Polyplex Stability via RiboGreen Binding

The stability of siRNA–polymer complexes was investigated with RiboGreen binding assay. First, the master mix of diluted genetic material and RiboGreen was prepared. In detail, 20 µg $mL^{-1}$ negative-control siRNA and 2 nmol $\mu L^{-1}$ RiboGreen were diluted in RNase-free HBG buffer and incubated in the dark for 10 min at room temperature. The polymers were diluted with RNase-free HBG buffer to give an N/P ratio of 20. An equal volume of master mix was added to the polymer solutions and the mixture was immediately vortexed at the highest speed for 3 s and incubated at room temperature for 15 min. Subsequently, after 15 min incubation, 10 µL of the polyplexes was added in triplicate for each formulation in a black 96-well plate. Following, 90 µL of RNase-free HBG buffer supplemented with 10% FBS and RNase-free buffer without FBS as the control was added to the polyplexes. The solution was mixed by resuspension before the fluorescence intensity was measured at $\lambda_{Ex} = 525$ nm/$\lambda_{Em} = 605$ nm. Afterward, the plate was incubated at 37 °C and measurement was repeated every 30 min. The result is shown in Figure S20 (Supporting Information). The percentage of siRNA release kinetic was calculated as follows

$$\text{rFI } [\%] = \frac{FI_{Sample} - FI_0}{FI_{siRNA} - FI_0} \times 100 \quad (5)$$

rFI is the relative fluorescence intensity, and $FI_{Sample}$, $FI_0$, and $FI_{siRNA}$ are the fluorescence intensities of the sample, of the blank, and the RiboGreen intercalated into genetic material (100%) of the first time point ($t = 0$ min incubation at 37 °C).


© 2023 The Authors. Macromolecular Bioscience published by Wiley-VCH GmbH

#### 2.2.10. Polyplex Preparation

The polyplexes were prepared with AllStars Neg. siRNA AF488 for uptake studies or GFP-22 siRNA and negative-control siRNA for knockdown studies. Polymers were diluted in RNase-free HBG buffer. The genetic material was then diluted in RNase-free HBG buffer and added 1:1 to the diluted polymer solution to match the targeted N/P ratio (Equation (S1), Supporting Information). Immediately, the solution was vortexed for 3 s at a maximum speed. The solution was incubated for 15 min at room temperature to ensure an efficient polyplex formation before being added to the cells.

#### 2.2.11. DLS of Polyplexes

Polyplexes were prepared as described in Section 2.2.10, and were measured with Zetasizer Ultra from Malvern Instruments. 70 µL of the samples were measured in disposable micro UV-Cuvettes. For each sample, 15 runs were performed (3 measurements and 5 runs per measurement) at 25 °C with measurement durations 0.839 s after an equilibration time of 30 s. General purpose was used as analysis model. A 633 nm He–Ne laser was used, and scattered light was detected at a backscattering angle of 173°. The size distribution by intensity was used to calculate the hydrodynamic diameter of the polyplexes. The result is shown in Figure S21 (Supporting Information).

#### 2.2.12. Particle Uptake Study

HEK293T, MCF-7, and MDA-MB-231 cell lines were treated with 50 µL of AllStars Neg AF488-siRNA–polymer complexes for the particle uptake studies. The uptake was performed over 4 h (Supporting Information) and 24 h to check the specificity of the particle uptake. The assay was performed in full growth medium supplemented with 10% FBS and 10 mM HEPES (D10H). After the incubation, cells were washed twice with warm PBS, detached by adding trypsin–EDTA, incubated for 10 min, then resuspended in fresh D10. 250 µL of cell suspension were transferred to a 96-well plate. The AF488 signal was measured via flow cytometry (Cytoflex S, Beckmann Coulter, Brea, CA, USA) at $\lambda_{Ex} = 488$ nm combined with a 525/40 nm bandpass filter (fluorescein isothiocyanate (FITC) channel). Viable single cells were gated according to the forward scatter/side scatter (FSC/SSC) pattern of the untreated control. AF488 positive cells were gated to the master mix (Figure S1, Supporting Information). The relative mean fluorescence intensity (rMFI) of viable single cells was calculated relative to the master mix with noncomplexed siRNA (rMFI singlets) and to the reference bPEI that was used for the synthesis of the respective polymer sample (rMFI to ref)

$$\text{rMFI singlets} = \frac{FI_{singlets}}{FI_{MM}} \tag{6}$$

$$\text{rMFI to ref} = \frac{FI_{singlets}}{FI_{bPEI}} \tag{7}$$

$FI_{singlets}$, $FI_{MM}$, and $FI_{bPEI}$ are the fluorescence intensities of viable single cells treated with siRNA–polymer complexes, with free noncomplexed siRNA, and with siRNA–bPEI complexes, respectively.

#### 2.2.13. Particle Uptake Inhibition Study with MSNBA

The assay was performed according to a literature procedure.[45] Polyplexes of **Fru1(80)−10bPEI** were prepared as described in Section 2.2.10. One hour after medium change to 450 µL D10H, MDA-MB-231, MCF-7, and HEK293T were treated with 25 µM MSNBA for 15 min. Polyplexes were added and cells were incubated for further 15 min. For harvesting, cells were washed twice with PBS, and trypsinated for 10 min before resuspended in D10. Cell suspension was transferred to a 96-well plate to measure the particle uptake by flow cytometry. The result is shown in Figure S25 (Supporting Information).

#### 2.2.14. Knockdown Study

To study the knockdown potential, leading polymers were complexed with GFP-22 siRNA, or with negative-control siRNA for the negative control. The assay was performed in HEK293-GFP and MDA-MB-231-GFP cell lines to prove the specificity of the formulation. For this, cells were incubated with 50 µL of formed polyplex solutions (N/P 20 and 2 µg mL$^{-1}$ of genetic material on cells) for 24 h. Afterward, the old medium was replaced by fresh D10H, and cells were further incubated for another 48 h before harvesting. After 24+48 h incubation, cells were washed twice with PBS, detached with trypsin–EDTA, and resuspended in new D10. The cell suspension was transferred to a 96-well plate, and the GFP signal was measured via flow cytometry (Cytoflex, Beckmann Coulter, Brea, CA, USA) at $\lambda_{Ex} = 488$ nm combined with a 525/40 nm bandpass filter (FITC channel). Viable single cells were gated according to the FSC/SSC pattern of the untreated control, and GFP-knockdowned cells were gated to the negative control (treated with negative-control siRNA). The knockdown efficiency was calculated as follows

$$\text{Knockdown efficiency } [\%] = \frac{FI_{Ctrl} - FI_{Sample}}{FI_{Ctrl}} \times 100 \tag{8}$$

$FI_{Ctrl}$ and $FI_{Sample}$ are the fluorescence intensities of viable single cells treated with negative-control siRNA–polymer complexes and GFP-22 siRNA–polymer complexes, respectively.

#### 2.2.15. Statistical Analysis

All determinations were made at least in triplicate, and data were reported as mean ± standard deviation (SD). Statistical analyses were calculated using OriginPro2022b software. The one-way analysis of variance (ANOVA) was applied to determine the statistical significance. If a statistically significant difference is given ($p \leq 0.05$), Bonferroni's posthoc test was performed. Statistical significance was notated as $^{*}p \leq 0.05$,$^{**}p \leq 0.01$, and $^{***}p < 0.001$.

## 3. Results and Discussion

Amines readily react with primary epoxides in an $S_N2$-reaction, forming $\beta$-amino alcohols in high yields.[46] This reaction


© 2023 The Authors. Macromolecular Bioscience published by Wiley-VCH GmbH

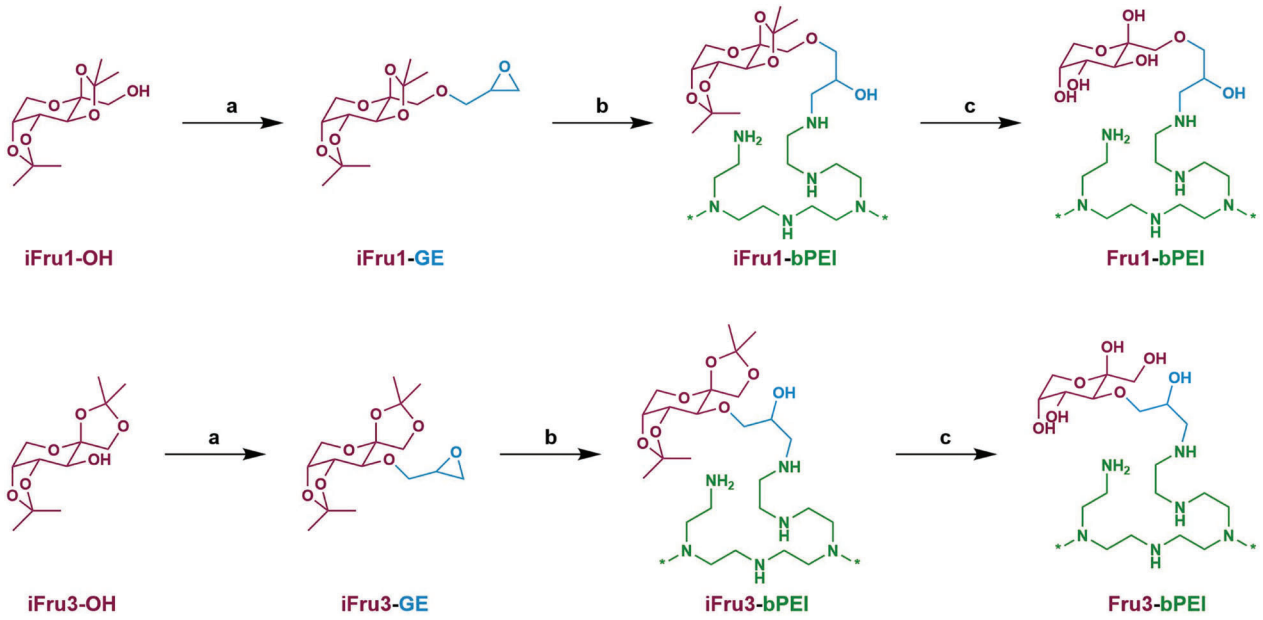


**Scheme 1.** Synthesis of Fru–bPEIs. a) epichlorohydrin, TBAI, THF/NaOH, 50 °C. b) bPEI, MeOH, 40 °C; c) TFA/$H_2O$, RT.

proceeds under mild conditions, generates no additional side products, and tolerates the presence of both alcohols and water under basic conditions as provided by bPEI.

In the scope of this work, conjugation via both the C1 and C3 positions of D-fructose was investigated. The two precursors are both accessible via the protection of D-fructose with acetone under acidic conditions, wherein 1,2:4,5-di-*O*-isopropylidene-*β*-D-fructopyranoside (**iFru3–OH**) is formed as the kinetic product, and 2,3:4,5-di-*O*-isopropylidene-*β*-D-fructopyranoside (**iFru1–OH**) is the thermodynamic product.[43]

### 3.1. Synthesis of Epoxide-Functionalized D-Fructoses

These two compounds were converted into glycidyl ethers by reacting their free hydroxyl groups with epichlorohydrin in THF/aq. NaOH under phase transfer catalysis (PTC) conditions using TBAI as catalyst (**Scheme 1**a). Both products **iFru1–GE** and **iFru3–GE** were obtained in good yields of 70–80%.

The synthesis of **iFru1–GE** was initially attempted in the absence of water (NaH in dry THF under argon). These conditions gave lower yields and promoted an unwanted side reaction where epichlorohydrin was converted into di(3-glycidyloxy-prop-1-en-1-yl) ether, which had previously only been reported to form under PTC conditions ($^1$H-NMR spectrum; Figure S7, Supporting Information).[47] This led us to favor THF/aq. NaOH for the synthesis of fructose epoxides, where only small amounts of the side product formed that could be separated with flash chromatography.

**Figure 2** shows the $^1$H-NMR spectra of protected *β*-D-fructopyranoses and their glycidyl ethers. The OH-signals of the educts at 2.26 ppm (iFru1) and 2.09 ppm (iFru3) have disappeared, while new signals belonging to the epoxide ring system appeared in the range 3.2–2.5 ppm. This confirms the successful introduction of the glycidyl ether moiety. Because

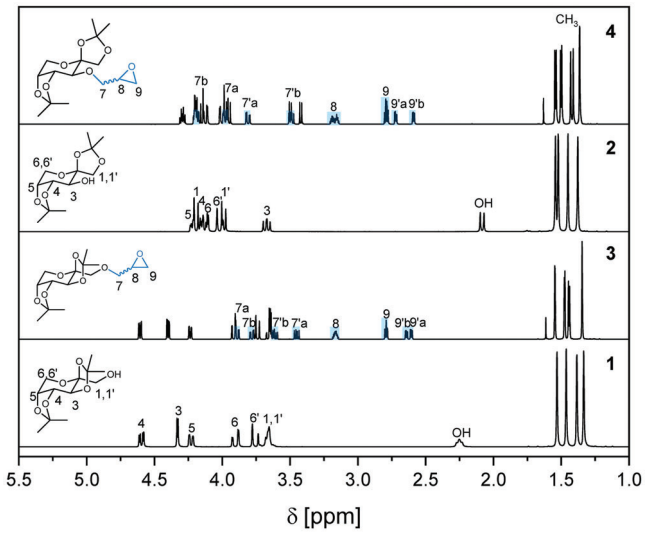


**Figure 2.** $^1$H-NMR spectra of (top to bottom) **iFru3-GE**, **iFru3-OH**, **iFru1–GE**, and **iFru1–OH** (300 or 500 MHz, $CDCl_3$).

racemic epichlorohydrin was used for the synthesis, the products **iFru1–GE** and **iFru3–GE** were obtained as a mixture of two diastereomers (a and b). This causes most signals to appear doubled, with shift differences increasing near the epoxide ring (most notably H7 and H9). $^{13}$C-NMR spectra likewise show two signals for each carbon atom. Signals were assigned to their respective diastereomers wherever possible.

### 3.2. Synthesis of D-Fructose-Functionalized bPEI (Fru–bPEI)

Isopropylidene-protected D-fructose-functionalized bPEIs (iFru–bPEIs) were obtained by reaction of the glycidyl ethers


© 2023 The Authors. Macromolecular Bioscience published by Wiley-VCH GmbH

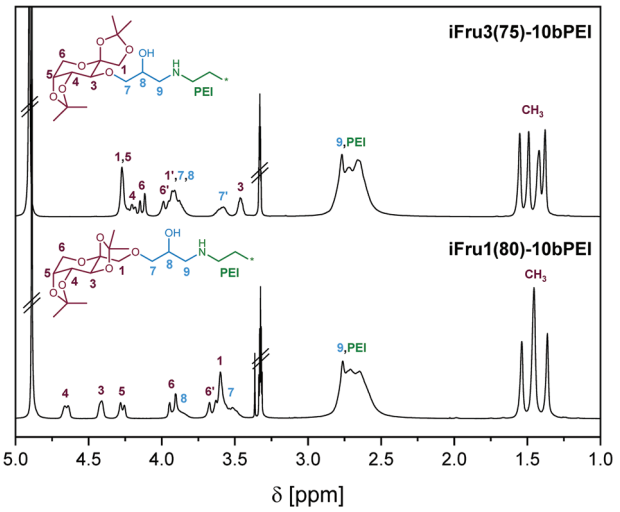


**Figure 3.** $^{1}$H-NMR spectra of iFru–bPEIs (400 MHz, $CDCl_3$).

**iFru1–GE** and **iFru3–GE** with commercially available bPEI of molecular weights 1.8 and 10 kDa (**1.8bPEI** and **10bPEI**) in methanol at 40–50 °C (Scheme 1b). We wanted to investigate the influence of molecular weight, degree of substitution, and linker position (linker on C1 versus linker on C3 of D-fructose) on the suitability of Fru–bPEI for gene delivery applications. For this purpose, a small library of polymers was prepared from **10bPEI** using varying ratios of **iFru1–GE** to produce iFru1–10bPEIs with different pDS. In addition, samples of iFru1–1.8bPEI, iFru3-1.8bPEI, and iFru3-10bPEI with a similar pDS of ≈80% are prepared (Table 1). An intermediate pDS was chosen for these samples because it allows the polymers to carry a lot of D-fructose moieties for GLUT5-targeting while leaving some primary amines unfunctionalized to interact with siRNA.

Because the glycidyl ethers react much faster with primary amines than with secondary amines, the degrees of substitution in this work are expressed relative to the primary amine groups of bPEI. The ratio of primary:secondary:tertiary amines in commercial bPEI is ≈1:1:1 (verified by inverse-gated $^{13}$C-NMR spectroscopy).[48] Consequently, the total DS can be inferred by simply dividing the pDS by 3.

The functionalization works well up to a pDS of 100%, then becomes increasingly inefficient as less accessible secondary amines need to react with the relatively bulky D-fructose epoxides. With the addition of an excess of **iFru1–GE**, a pDS of 190% was reached after 14 days, out of a theoretical maximum of 300% (double substitution on primary amines and single substitution on secondary amines). Reaction control via $^{1}$H-NMR also shows significantly faster conversion of the epoxides with **1.8bPEI** (2–3 days until completion) compared to **10bPEI** (10–14 days until completion).

**Figure 3** shows the $^{1}$H-NMR characterization of two iFru–bPEIs synthesized from 10 kDa bPEI with a pDS of ≈80% (spectra of all protected polymers; Figure S11, Supporting Information). The successful functionalization of bPEI is confirmed by signals of D-fructose in the 4.7–3.4 ppm range as well as isopropylidene signals at 1.7–1.2 ppm.

**Table 3.** Molar masses of bPEI and Fru–bPEIs as determined by SEC (0.1% TFA in 0.1 M NaCl). Bracketed results were measured after storage at room temperature for several weeks.

| Name | $M_n$ [g mol$^{-1}$] | $Đ$ |
|---|---|---|
| **1.8bPEI** | 1370 | 1.7 |
| **10bPEI** | 5150 | 2.0 |
| **Fru1(80)–1.8bPEI** | 1480 (1980) | 1.7 (1.7) |
| **Fru3(85)–1.8bPEI** | 1420 (2240) | 1.8 (7.6) |
| **Fru1(30)–10bPEI** | 10 250 | 1.2 |
| **Fru1(55)–10bPEI** | 9590 | 1.3 |
| **Fru1(80)–10bPEI** | 10 620 | 1.5 |
| **Fru1(110)–10bPEI** | 10 170 | 1.3 |
| **Fru1(190)–10bPEI** | 9550 | 1.4 |
| **Fru3(80)–10bPEI** | 11 370 (17 910) | 2.4 (2.0) |

The isopropylidene-protected polymers were deprotected in a mixture of TFA in water, which was chosen because deprotection can be achieved quickly at room temperature (> 98% conversion after 5 h). By comparison, deprotection in dilute HCl was still incomplete after 8 days. After precipitation, the deprotected polymers still contained substantial amounts of trifluoroacetate as counterion to the protonated amines of bPEI, which needed to be removed due to its toxicity. This was accomplished via salt exchange by repeated dialysis in excess PBS buffer, which has the additional benefit of neutralizing the acidic polymers to a physiological pH of 7.4. The salt exchange with PBS led to Fru–bPEIs containing hydrogen phosphates and chloride as counterions on protonated amines. In some samples, an additional salt exchange was performed in NaCl solution to yield Fru–bPEIs containing only chloride as counterion.

NMR analysis confirms the successful deprotection of D-fructose moieties by disappearance of the isopropylidene signals at 1.7–1.2 ppm. Signals belonging to D-fructose are found overlapping in a broad range of 4.25–3.0 ppm. The deprotection of the C2 position allows the pyranose ring of D-fructose to open, leading to a mixture of different isomers. $^{13}$C-NMR and rapid heteronuclear single quantum correlation (ASAP-HSQC) NMR spectroscopy[49] of D-fructose-functionalized 1.8bPEIs (Figure 1; Figure S13, Supporting Information) confirm the presence of $\beta$-pyranose, $\beta$-furanose, and $\alpha$-furanose isomers (in order of decreasing content). Only $^{1}$H-NMR spectra (Figure S12, Supporting Information) are presented for the larger Fru–10bPEIs because of their lower solubility.

Fru–bPEIs were analyzed with SEC (**Table 3** and **Figure 4**). While interactions with the column material and the lack of a suitable calibration standard for bPEI make it difficult to determine accurate molar masses via SEC, the technique is still suitable for comparing samples to each other by their hydrodynamic radius. All D-fructose-substituted bPEIs show a slightly lower elution volume than their unfunctionalized counterparts, corresponding to an increased hydrodynamic radius and, consequently, higher molar mass. However, the size difference is smaller than expected, given the high D-fructose content. There is no apparent correlation between D-fructose content and molar mass in Fru1–10bPEIs (Figure 4B), which suggests that additional D-fructose either does not increase the hydrodynamic ra-


© 2023 The Authors. Macromolecular Bioscience published by Wiley-VCH GmbH

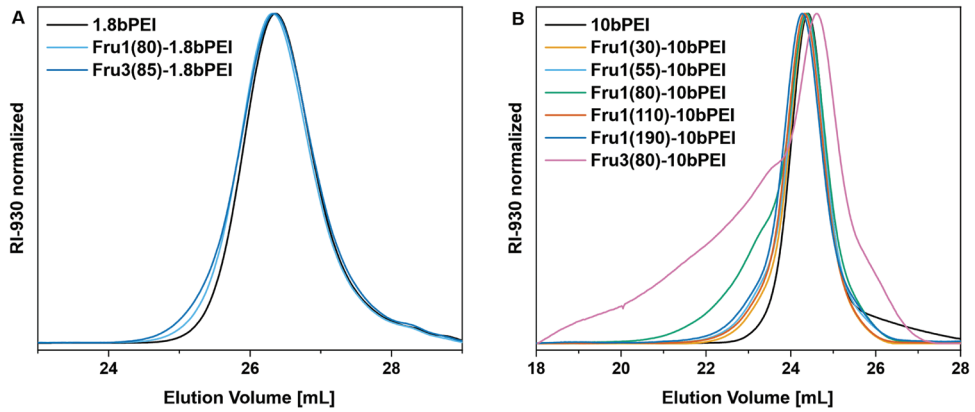


**Figure 4.** SEC data of D-fructose-substituted bPEIs. A) 1.8 kDa. B) 10 kDa.

dius significantly or changes the interaction with the column in such a way that the difference is not detected by SEC.

The obtained polymers are water soluble and mostly insoluble in organic solvents. Samples stored at room temperature (RT) for several weeks show a color change and decreasing water solubility, suggesting that the polymers are unstable under these conditions. SEC analysis of samples after extended storage at RT shows an increase in molar mass (Table 3; Figure S16, Supporting Information). This indicates that Fru–bPEIs undergo crosslinking reactions at room temperature, leading to the formation of larger polymer species. These crosslinking reactions are much more prevalent if D-fructose is conjugated via C3 instead of C1, and **Fru3(80)–10bPEI** even shows crosslinking right after synthesis. An explanation for this could be the formation of imine linkages between amines of bPEI and the carbonyl group of open-chain D-fructose. Conjugation via C3 allows the sugar to isomerize and form a more reactive open-chain aldehyde, while only the less reactive ketone is accessible if C1 is "locked" by the attached linker. No noticeable changes in the polymers were observed after several months of storage in a freezer, suggesting that Fru–bPEIs are stable at −20 °C.

### 3.3. Cytotoxicity Study

The potential of bPEI as a nonviral gene carrier is limited by its cytotoxicity, which increases drastically with increasing molecular weight. To test if D-fructose substitution can provide substantial improvements, cytotoxicity screening of different Fru–bPEIs was performed with L929 cells as recommended by ISO10993-5. The PrestoBlue assay was applied to determine the relative metabolic activity, which correlates with cell viability.

**Figure 5** shows the PrestoBlue assay of **10bPEI** and different Fru–10bPEIs. **10bPEI** clearly shows decreasing cell viability at higher polymer concentration, with a 50% cytotoxicity concentration (CC50) value of 10.4 µg mL$^{-1}$. Due to its high cytotoxicity, **10bPEI** was only tested up to 50 µg mL$^{-1}$. At this concentration, cytotoxicity of all Fru1–10bPEIs is significantly lower compared to unsubstituted **10bPEI** ($p < 0.001$). Fru1–10bPEIs also show little to no cytotoxicity at higher concentrations of up to 500 µg mL$^{-1}$. Only **Fru1(30)–10bPEI** is slightly cytotoxic with a metabolic activity below 70% at 500 µg mL$^{-1}$. The results demonstrate that D-fructose substitution greatly improves the biocompatibility of bPEI, reducing cytotoxicity significantly at low degrees of substitution and even more with increasing D-fructose content. Observations of **1.8bPEI** and its D-fructose substituted derivatives gave similar results, though the difference is less drastic because of the lower toxicity of **1.8bPEI** (Figure S17, Supporting Information).

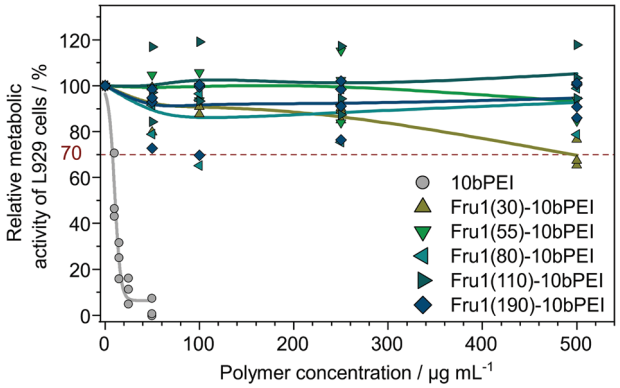


**Figure 5.** Metabolic activity (PrestoBlue assay) in L929 cells incubated with Fru1–10bPEIs in full growth medium (D10) for 24 h. Single repetitions are represented in dots, and lines are fitted with the dose-respond function ($n = 3$). A relative metabolic activity below 70% is considered cytotoxic.

### 3.4. Investigation of siRNA–Polyplex Formation with Fru–bPEIs

Successful polyplex formation and protection against degradation is a crucial first step for effective gene delivery. Due to the high positive charge density of bPEI, it can condensate negatively charged genetic material through electrostatic interactions to form stable polyplexes.

Polyplexes of siRNA (N/P = 20) with Fru1–10bPEIs at different pDS were investigated with DLS (Figure S18 and Table S2, Supporting Information). Thus, it could be shown that **10bPEI** forms polyplexes with an average size of 53 nm. Fru–bPEIs with low pDS (30% and 55%) form polyplexes with a larger average hydrodynamic radius of 95 nm (intensity maximum at 130 nm). At high pDS (80% and 110%), signal intensity decreases and


© 2023 The Authors. Macromolecular Bioscience published by Wiley-VCH GmbH

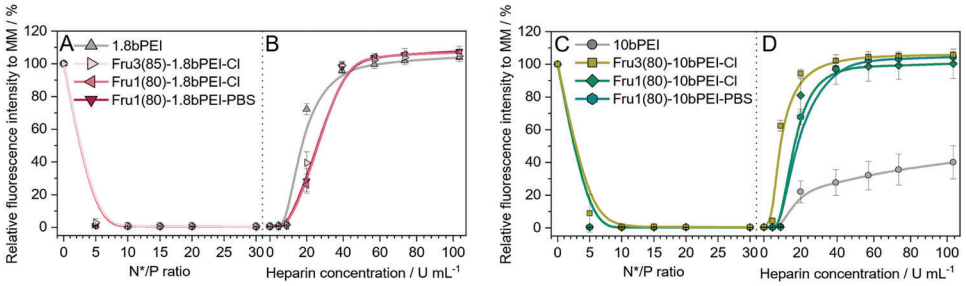


**Figure 6.** A,C) RiboGreen binding assays, and B,D) heparin release assays at N/P 20 for D-fructose-conjugated bPEIs. Single repetitions are represented as dots, and lines were fitted using a logistic function ($n = 3$).

the particle size distribution is no longer unimodal (high PDI), with smaller structures in the 10–40 nm range being dominant. This is likely advantageous because smaller particles can be preferentially taken up by cells and can penetrate deep into the tissue for cancer therapy.[51,52] One potential explanation is that Fru–bPEI has fewer accessible binding sites for siRNA at high pDS, leading to the formation of diffuse aggregates with less interconnection between RNA strands, thus forming fewer well-defined condensed polyplexes. Such diffuse morphologies are difficult to characterize accurately by DLS or electron microscopy and were also observed in other studies using bPEI–siRNA polyplexes.[24,53]

A RiboGreen binding assay was performed with **1.8bPEI** (**Figure 6A**) and **10bPEI** (Figure 6C) as well as their D-fructose substituted derivatives at pDS 80%. The assay is based on a change in the fluorescent intensity of RiboGreen when intercalated with genetic material. Upon polymer addition, the electrostatic and hydrophobic interactions between the polymer and siRNA lead to displacement of intercalated RiboGreen, resulting in a decreased fluorescence intensity.

Due to the sharp decrease of fluorescence intensity at all tested N/P ratios, it can be concluded that all tested polymers have a high affinity for siRNA complexation, irrespective of their molecular weight or counterion. There appears to be little to no difference in siRNA-binding if D-fructose is conjugated via the C3 position instead of C1. The assay for **10bPEI** and **Fru1(80)–10bPEI** was additionally performed at N/P ratios ≤ 5 (Figure S19A, Supporting Information), revealing a nearly 100% reduction of fluorescence intensity even at N/P = 1, which further demonstrates their high affinity for siRNA complexation. The stability of Fru–bPEI–siRNA polyplexes at N/P = 20 was further studied over time in RNase-free HBG buffer as well as HBG buffer with 10% serum proteins at 37 °C (Figure S21, Supporting Information). At $t = 0$ min, all tested polymers fully complex siRNA even in the presence of serum. After 4 h, noncomplexed siRNA completely degraded in the presence of serum, while no release of siRNA from Fru–bPEI polyplexes is observed. This demonstrates that Fru–bPEI forms polyplexes in the presence of serum and that these polyplexes are sufficiently stable over time.

For effective gene delivery, complexation is only the first step. Once delivered to the site of action, the polyplex also has to be able to release its cargo. The release properties of siRNA polyplexes at N/P = 20 were tested by adding the polyanionic competitor heparin, a polysaccharide from the extracellular matrix (Figure 6B,D). Heparin binds strongly to bPEI and displaces siRNA from the polyplex, allowing RiboGreen to re-intercalate into the released siRNA. The resulting increase in fluorescence intensity is proportional to the amount of released siRNA. All D-fructose substituted bPEIs and **1.8bPEI** already show high fluorescence intensity at low heparin concentrations, indicating a rapid release. In comparison, **10bPEI** has a stronger affinity to genetic material, releasing only up to 40% of genetic material at the tested heparin concentrations due to its high charge density. The incorporation of D-fructose into bPEI sterically blocks access to the polyamine backbone and reduces the positive charge density, supporting siRNA release.

To sum up, all polymers revealed a high affinity for the complexation of siRNA even at low N/P ratios. Unlike pure bPEI, Fru–bPEIs released almost all genetic material rapidly at a heparin concentration of 40 U $mL^{-1}$. Remarkably, Fru–bPEI polyplexes did not demonstrate a strong dependency on molecular weight compared to the reference **1.8bPEI** and **10bPEI**. Furthermore, the substitution position and the counterion type have minimal effects on polyplex formation and siRNA release.

### 3.5. Investigation of Cell-Type-Specific Particle Uptake

Uptake efficiency and specificity of Fru–bPEI–siRNA polyplexes was studied on the GLUT5-overexpressing triple-negative breast cancer cell line MDA-MB-231, with HEK293T as a control cell line. The experiments were performed with siRNA labeled with Alexa Fluor 488. Polyplex uptake is indicated by detection of fluorescence in viable, single cells (AF488 pos cells). The quantity of siRNA uptake correlates with their rMFI singlets (Figure S23, Supporting Information). Improvements in uptake due to incorporation of D-fructose are illustrated by the mean fluorescence intensity after exposure to Fru–bPEI polyplexes relative to bPEI polyplexes (rMFI to ref, **Figure 7**A).

Figure 7A (left) shows 100% AF488 positive cells in both cell lines for **10bPEI** and for all Fru–10bPEIs except **Fru1(190)–10bPEI**. Only 50–70% of cells are AF488 positive for **1.8bPEI** and close to no fluorescent cells are detected for Fru–1.8bPEIs, demonstrating the strong influence of molecular weight on siRNA polyplex uptake. A comparison of rMFI values for Fru–10bPEIs (rMFI singlets; Figure S23, Supporting Information) shows higher fluorescent intensity in MDA-MB-231 than in the control cell line. Significant selectivity for MDA-MB-231 cell line was observed for samples with pDS 55–80% ($p <$


© 2023 The Authors. Macromolecular Bioscience published by Wiley-VCH GmbH

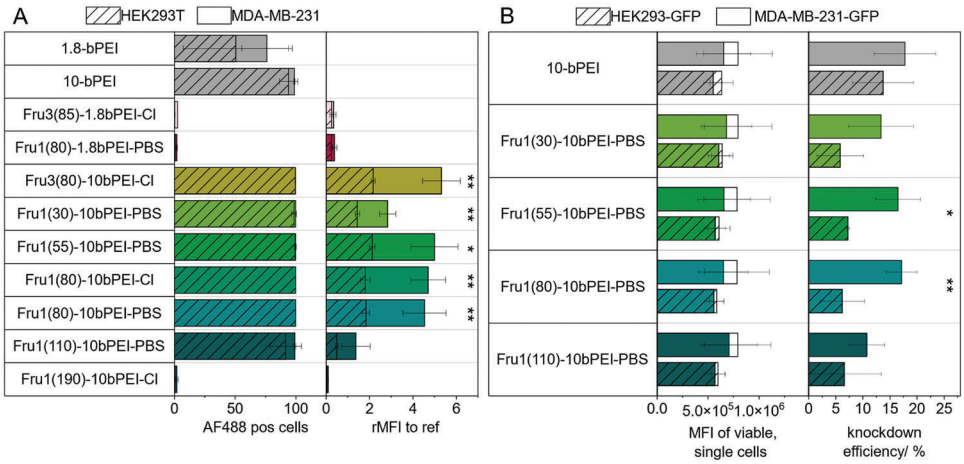


**Figure 7.** A) Uptake efficiency tests of bPEI- and Fru–bPEI polyplexes with Alexa Fluor-labeled siRNA (AllStars Neg. siRNA AF488), performed in HEK293T and MDA-MB-231 cell lines in full growth medium supplemented with 10% FBS and 10 mM HEPES (D10H) over 24 h. B) Knockdown efficiency assay of 10 kDa bPEI with different pDS of D-fructose, performed in HEK293-GFP and MDA-MB-231-GFP cell lines in D10H over 24 h followed by medium change and further incubation for 48 h. MFI values with GFP-22-siRNA polyplexes are represented as color bars, and colorless parts illustrate the knockdown compared to negative-control siRNA polyplexes. Significant differences in uptake between HEK293T and MDA-MB-231 and knockdown efficiency between HEK293-GFP and MDA-MB-231-GFP cell lines are illustrated as $*p < 0.05$, $**p < 0.01$. Values represent mean ± SD ($n \geq 3$). Both assays were analyzed via flow cytometry.

0.05), while **10bPEI** performed better in the HEK293T cell line ($p < 0.01$).

In comparison to **10bPEI** (rMFI to ref, Figure 7A), D-fructose-conjugation enhances uptake approximately fivefold in MDA-MB-231 breast cancer cells and twofold in control cells (**Fru1(55)–10bPEI**, **Fru1(80)–10bPEI**, and **Fru3(80)–10bPEI**). Less substituted **Fru1(30)–10bPEI** shows lower improvements in uptake efficiency, especially in breast cancer cells. However, a high pDS above 100% is clearly also very disadvantageous for siRNA uptake, highlighting the importance of having both D-fructose moieties and some unfunctionalized primary amines in the polymer. The uptake efficiency and specificity are unaffected by the chosen counterions (**Fru1(80)–10bPEI–Cl** and **Fru1(80)–10bPEI–PBS**). Notably, no significant difference between substitution via C1 and C3 was observed, with **Fru3(80)–10bPEI** performing similarly to its Fru1 analogs. Both variants are able to effectively target MDA-MB-231 cells, but substitution via C1 is preferable due to the increased storage stability of Fru1-bPEIs. The high uptake of **Fru3(80)–10bPEI** could also be partially explained by its slightly higher molecular weight as a result of crosslinking. Over 24 h, cell specificity for MDA-MB-231 cells is achieved, whereas HEK293T cells initially show higher uptake after a short incubation time of 4 h (Figure S22, Supporting Information), but with no further increase in uptake efficiency over time.

An additional uptake study with **Fru1(80)–10bPEI** was performed in the human breast cancer cell line MCF-7 (Figure S24, Supporting Information). Surprisingly, no significant increase in uptake of fructose-functionalized polyplexes over **10bPEI** polyplexes was observed in MCF-7 cells. To gain more insight into the uptake mechanism, an inhibition assay was performed in which MSNBA was added as an inhibitor to the GLUT5 transporter (Figure S25, Supporting Information).[45] GLUT5 inhibition results in a significantly lower uptake in MDA-MB-231, demonstrating that GLUT5-mediated endocytosis plays a major role in the specific uptake of Fru–bPEI–siRNA polyplexes in triple-negative breast cancer cells. No uptake decrease was observed as a result of GLUT5 inhibition in MCF-7 and the control cell line HEK293T. While most literature sources observe GLUT5-mediated uptake into MCF-7 cells,[32] low GLUT5 expression in MCF-7 as well as a strong influence of culture conditions on GLUT5 expression levels have also been reported.[54,55] The results seem to indicate that our MCF-7 culture does not express enough GLUT5 to significantly influence Fru–bPEI uptake.

All in all, it can be concluded that D-fructose conjugation enhances the uptake efficiency of 10 kDa bPEI in MDA-MB-231 breast cancer cells up to more than fivefold, demonstrating the high uptake specificity of Fru–bPEIs. Higher degrees of substitution increase the uptake efficiency and specificity up to an optimum between pDS 55% and 80%, beyond which further D-fructose functionalization hinders siRNA polyplex uptake.

### 3.6. Investigation of Cell-Type-Specific Knockdown

To investigate whether Fru–bPEI polyplexes also achieve cell-specific transfection, knockdown experiments with GFP-22 siRNA were performed in MDA-MB-231-GFP cells and HEK293T-GFP cells (Figure 7B). Polyplexes of polymers that have shown little to no siRNA-uptake were not included in the knockdown experiment. Due to its tendency to crosslink, **Fru3(80)–10bPEI** was also excluded, and only 10 kDa bPEI with linker position on D-fructose via C1 and pDS ranging from 30% to 110% were investigated further.

The MFI of cells exposed to GFP–siRNA polyplexes is noticeably lower than the MFI of cells exposed to polyplexes of negative-control siRNA for all tested samples (difference illustrated by colorless area), proving a successful knockdown. Since the MFI of viable, single cells is strongly influenced by the cell type and


© 2023 The Authors. Macromolecular Bioscience published by Wiley-VCH GmbH

its GFP-protein expression rate, different cell lines cannot be directly compared by their fluorescent intensity. Therefore, only the relative MFI reduction in each cell line with GFP–siRNA versus negative-control siRNA is discussed (knockdown efficiency).

All Fru–bPEI-siRNA polyplexes demonstrate higher knockdown efficiency in the breast cancer cells, while the knockdown efficiency of **10bPEI**-siRNA polyplexes is comparable in both cell lines. Significant cell specificity for MDA-MB-231 is observed with **Fru1(55)–10bPEI** ($p < 0.05$) and high significance is observed with **Fru1(80)–10bPEI** ($p < 0.01$) with a knockdown efficiency up to 17% in MDA-MB-231 cells. Polyplexes of samples with pDS of 55% and 80%, which were identified as the most effective for siRNA uptake, are also found to be the most effective and specific formulations for siRNA-mediated knockdown. Both knockdown efficiency and specificity are reduced at a high pDS of 110% and at a low pDS of 30%, correlating with the previously observed lower siRNA uptake.

In conclusion, polyplexes of 10 kDa bPEI and its D-fructose conjugates can successfully provide transient knockdown of gene expression. Incorporating D-fructose at an intermediate pDS (55–80%) in the polymer structure can effectively target triple-negative breast cancer cells.

## 4. Conclusion

D-Fructose was successfully introduced to 1.8 and 10 kDa bPEI with varying degrees of substitution through different linker positions on D-fructose (C1 and C3), forming Fru–bPEIs. D-Fructose significantly improved biocompatibility of bPEI and functions as an effective targeting feature for triple-negative breast cancer. Despite the substitution with bulky D-fructose moieties, the affinity of Fru–bPEIs for the formation of siRNA polyplexes remains high even in the presence of serum, providing sufficient protection from degradation by RNases. At high pDS, the formed polyplexes are polydisperse, but mostly form nano-sized structures that are suitable for endocytosis (<100 nm). Fru–bPEI polyplexes also improve on bPEI in their ability to swiftly release genetic material under anion competition.

siRNA polyplexes of Fru–bPEIs were delivered specifically to triple-negative MDA-MB-231 breast cancer cells with five times higher siRNA uptake than polyplexes of bPEI, whereas uptake in HEK293T was only doubled. This specificity suggests a mechanism of receptor-mediated endocytosis, promoted by binding of D-fructose to the overexpressed transporter protein GLUT5. This is further supported by a decreasing uptake after MSNBA inhibition. The following knockdown experiments prove the efficacy of Fru–bPEI in RNAi applications, by showing similar knockdown capabilities to bPEI but with significantly improved target specificity. An intermediate degree of substitution (55–80% of primary amine groups) was found to be most effective in achieving high target specificity and knockdown efficiency.

In conclusion, D-fructose substituted bPEI is an effective vector for the delivery of siRNA into GLUT5-overexpressing cell lines. This gives it great potential for diagnostic and therapeutic applications, particularly for triple-negative breast cancer where existing treatment options are often ineffective. Good knockdown specificity of Fru–bPEI polyplexes was demonstrated, but the overall knockdown efficiency of 17% remains similar to bPEI. The presence of serum during incubation may partially explain the relatively low knockdown. For comparison, Dosta et al. analyzed the GFP knockdown of siRNA polyplexes with substituted cationic poly($\beta$-amino ester)s in MDA-MB-231 with and without preincubation in the presence of serum.[56] They reported that 24 h of polyplex preincubation in serum prevented knockdown with unfunctionalized polymer, but that partial modification with hydrophobic side chains alleviated the effect, allowing up to 50% knockdown efficiency with the best performer under identical conditions.

While achieving selective uptake and knockdown was the primary goal of this study, further modifications of the Fru–bPEI structure could be investigated in the future with the goal of improving knockdown efficiency. The aforementioned strategy of substituting cationic polymers with hydrophobic side chains could provide an effective way to increase knockdown efficiency of Fru–bPEI. Modification of bPEI with hydrophobic or anionic side chains has previously been shown to drastically change its interaction with membranes and genetic material, leading to better endosomal release and knockdown even at low degrees of substitution.[26,27] Because GLUT5 binding can potentially be adversely affected by substrate hydrophobicity,[57] the degree of substitution must be carefully balanced to avoid any adverse effects on the selectivity toward breast cancer cells.

## Supporting Information

Supporting Information is available from the Wiley Online Library or from the author.

## Acknowledgements

J.M.P. and L.S.R. contributed equally to this work. This study was funded by the AiF Projekt GmbH (ZiM-FuE-Kooperationsprojekt KK5064601). Further financial support from the Deutsche Forschungsgemeinschaft (DFG, German Research Foundation)—Project No. 316213987—SFB 1278 PolyTarget (Project Nos. B01 and C06), and the Bundesministerium für Bildung und Forschung (BMBF, Germany, #13XP5034A PolyBioMik) was acknowledged. The graphical abstract figure was created with BioRender.com.

Open access funding enabled and organized by Projekt DEAL.

## Conflict of Interest

The authors declare no conflict of interest.

## Data Availability Statement

The data that support the findings of this study are available from the corresponding author upon reasonable request.

## Keywords

bPEI, breast cancer, fructose, gene delivery, GLUT5, siRNA

Received: March 30, 2023
Revised: July 31, 2023
Published online: August 29, 2023


© 2023 The Authors. Macromolecular Bioscience published by Wiley-VCH GmbH

[1] R. L. Siegel, K. D. Miller, N. S. Wagle, A. Jemal, *Ca-Cancer J. Clin.* **2023**, *73*, 17.
[2] A. G. Waks, E. P. Winer, *JAMA, J. Am. Med. Assoc.* **2019**, *321*, 288.
[3] G. K. Gupta, A. L. Collier, D. Lee, R. A. Hoefer, V. Zheleva, L. L. Siewertsz Van Reesema, A. M. Tang-Tan, M. L. Guye, D. Z. Chang, J. S. Winston, B. Samli, R. J. Jansen, E. F. Petricoin, M. P. Goetz, H. D. Bear, A. H. Tang, *Cancers* **2020**, *12*, 2392.
[4] S. M. Elbashir, J. Harborth, W. Lendeckel, A. Yalcin, K. Weber, T. Tuschl, *Nature* **2001**, *411*, 494.
[5] A. Fire, S. Xu, M. K. Montgomery, S. A. Kostas, S. E. Driver, C. C. Mello, *Nature* **1998**, *391*, 806.
[6] B. Hu, L. Zhong, Y. Weng, L. Peng, Y. Huang, Y. Zhao, X.-J. Liang, *Signal Transduction Targeted Ther* **2020**, *5*, 101.
[7] M. Friedrich, A. Aigner, *BioDrugs* **2022**, *36*, 549.
[8] A. D. Springer, S. F. Dowdy, *Nucleic Acid Ther.* **2018**, *28*, 109.
[9] N. Sunaga, D. S. Shames, L. Girard, M. Peyton, J. E. Larsen, H. Imai, J. Soh, M. Sato, N. Yanagitani, K. Kaira, Y. Xie, A. F. Gazdar, M. Mori, J. D. Minna, *Mol. Cancer Ther.* **2011**, *10*, 336.
[10] W. Ngamcherdtrakul, D. S. Bejan, W. Cruz-Muñoz, M. Reda, H. Y. Zaidan, N. Siriwon, S. Marshall, R. Wang, M. A. Nelson, J. P. C. Rehwaldt, J. W. Gray, K. Hynynen, W. Yantasee, *Small* **2022**, *18*, 2107550.
[11] D. Kunze, K. Kraemer, K. Erdmann, M. Froehner, M. P. Wirth, S. Fuessel, *Int. J. Oncol.* **2012**, *41*, 1271.
[12] A. Basu, *Pharmacol. Ther.* **2022**, *230*, 107943.
[13] V. Pileczki, L. Pop, C. Braicu, L. Budisan, G. Bolba Morar, P. Del C Monroig-Bosque, R. V. Sandulescu, I. Berindan-Neagoe, *OncoTargets Ther.* **2016**, *9*, 6921.
[14] T.-H. Lee, S. Seng, M. Sekine, C. Hinton, Y. Fu, H. K. Avraham, S. Avraham, *PLoS Med.* **2007**, *4*, e186.
[15] M. Saraswathy, S. Gong, *Mater. Today* **2014**, *17*, 298.
[16] A. Babu, A. Munshi, R. Ramesh, *Drug Dev. Ind. Pharm.* **2017**, *43*, 1391.
[17] D. M. Dykxhoorn, D. Palliser, J. Lieberman, *Gene Ther.* **2006**, *13*, 541.
[18] A. L. Jackson, P. S. Linsley, *Nat. Rev. Drug Discovery* **2010**, *9*, 57.
[19] A. Singh, P. Trivedi, N. K. Jain, *Artif. Cells Nanomed. Biotechnol.* **2018**, *46*, 274.
[20] H. Yin, R. L. Kanasty, A. A. Eltoukhy, A. J. Vegas, J. R. Dorkin, D. G. Anderson, *Nat. Rev. Genet.* **2014**, *15*, 541.
[21] S. Nimesh, *Curr. Clin. Pharmacol.* **2012**, *7*, 121.
[22] S. Höbel, A. Aigner, *Wiley Interdiscip. Rev.: Nanomed. Nanobiotechnol.* **2013**, *5*, 484.
[23] O. Boussif, F. Lezoualc'h, M. A. Zanta, M. D. Mergny, D. Scherman, B. Demeneix, J. P. Behr, *Proc. Natl. Acad. Sci. USA* **1995**, *92*, 7297.
[24] M. Wagner, A. C. Rinkenauer, A. Schallon, U. S. Schubert, *RSC Adv.* **2013**, *3*, 12774.
[25] O. M. Merkel, A. Beyerle, D. Librizzi, A. Pfestroff, T. M. Behr, B. Sproat, P. J. Barth, T. Kissel, *Mol. Pharmaceutics* **2009**, *6*, 1246.
[26] W. Shen, H. Wang, Y. Ling-Hu, J. Lv, H. Chang, Y. Cheng, *J. Mater. Chem. B* **2016**, *4*, 6468.
[27] A. Zintchenko, A. Philipp, A. Dehshahri, E. Wagner, *Bioconjugate Chem.* **2008**, *19*, 1448.
[28] B. Liang, M.-L. He, C.-Y. Chan, Y.-C. Chen, X.-P. Li, Y. Li, D. Zheng, M. C. Lin, H.-F. Kung, X.-T. Shuai, Y. Peng, *Biomaterials* **2009**, *30*, 4014.
[29] R. Kircheis, L. Wightman, A. Schreiber, B. Robitza, V. Rössler, M. Kursa, E. Wagner, *Gene Ther.* **2001**, *8*, 28.
[30] G. Jiang, K. Park, J. Kim, K. S. Kim, S. K. Hahn, *Mol. Pharmaceutics* **2009**, *6*, 727.
[31] H.-L. Jiang, Y.-K. Kim, R. Arote, J.-W. Nah, M.-H. Cho, Y.-J. Choi, T. Akaike, C.-S. Cho, *J. Controlled Release* **2007**, *117*, 273.
[32] M. H. Stenzel, *Macromolecules* **2022**, *55*, 4867.
[33] S. P. Zamora-León, D. W. Golde, I. I. Concha, C. I. Rivas, F. Delgado-López, J. Baselga, F. Nualart, J. C. Vera, *Proc. Natl. Acad. Sci. USA* **1996**, *93*, 1847.
[34] A. Godoy, V. Ulloa, F. Rodríguez, K. Reinicke, A. J. Yañez, M. D. L. A. García, R. A. Medina, M. Carrasco, S. Barberis, T. Castro, F. Martínez, X. Koch, J. C. Vera, M. T. Poblete, C. D. Figueroa, B. Peruzzo, F. Pérez, F. Nualart, *J. Cell. Physiol.* **2006**, *207*, 614.
[35] M. Wuest, I. Hamann, V. Bouvet, D. Glubrecht, A. Marshall, B. Trayner, O.-M. Soueidan, D. Krys, M. Wagner, C. Cheeseman, F. West, F. Wuest, *Mol. Pharmacol.* **2018**, *93*, 79.
[36] C. Cao, J. Zhao, M. Lu, C. J. Garvey, M. H. Stenzel, *Biomacromolecules* **2019**, *20*, 1545.
[37] J. Zhao, M. Lu, H. Lai, H. Lu, J. Lalevée, C. Barner-Kowollik, M. H. Stenzel, P. Xiao, *Biomacromolecules* **2018**, *19*, 481.
[38] P. S. Omurtag Ozgen, S. Atasoy, B. Zengin Kurt, Z. Durmus, G. Yigit, A. Dag, *J. Mater. Chem. B* **2020**, *8*, 3123.
[39] C. Englert, M. Pröhl, J. A. Czaplewska, C. Fritzsche, E. Preußger, U. S. Schubert, A. Traeger, M. Gottschaldt, *Macromol. Biosci.* **2017**, *17*, 1600502.
[40] T. Bus, C. Englert, M. Reifarth, P. Borchers, M. Hartlieb, A. Vollrath, S. Hoeppener, A. Traeger, U. S. Schubert, *J. Mater. Chem. B* **2017**, *5*, 1258.
[41] A. Kwok, S. L. Hart, *Nanomedicine* **2011**, *7*, 210.
[42] "AAT Bioquest Inc., Quest Calculate PBS (Phosphate Buffered Saline) (1X, pH 7.4) Preparation and Recipe, https://www.aatbio.com/resources/buffer-preparations-and-recipes/pbs-phosphate-buffered-saline (accessed: 15 June 2021).
[43] R. F. Brady, *Carbohydr. Res.* **1970**, *15*, 35.
[44] N. Tewari, V. K. Tiwari, R. P. Tripathi, V. Chaturvedi, A. Srivastava, R. Srivastava, P. K. Shukla, A. K. Chaturvedi, A. Gaikwad, S. Sinha, B. S. Srivastava, *Bioorg. Med. Chem. Lett.* **2004**, *14*, 329.
[45] N. Gora, L. J. Weselinski, V. V. Begoyan, A. Cooper, J.-Y. Choe, M. Tanasova, *ACS Chem. Biol.* **2023**, *18*, 1089.
[46] S. J. Stropoli, M. J. Elrod, *J. Phys. Chem. A* **2015**, *119*, 10181.
[47] Y. Yao, Z. Li, Y. Qiu, J. Bai, J. Su, D. Zhang, S. Jiang, *Sci. Rep.* **2015**, *5*, 14231.
[48] A. Von Harpe, H. Petersen, Y. Li, T. Kissel, *J. Controlled Release* **2000**, *69*, 309.
[49] D. Schulze-Sünninghausen, J. Becker, M. R. M. Koos, B. Luy, *J. Magn. Reson.* **2017**, *281*, 151.
[50] C. Colombo, C. Aupic, A. R. Lewis, B. M. Pinto, *J. Agric. Food Chem.* **2015**, *63*, 8551.
[51] P. Foroozandeh, A. A. Aziz, *Nanoscale Res. Lett.* **2018**, *13*, 339.
[52] A. Tchoryk, V. Taresco, R. H. Argent, M. Ashford, P. R. Gellert, S. Stolnik, A. Grabowska, M. C. Garnett, *Bioconjugate Chem.* **2019**, *30*, 1371.
[53] M. Zheng, G. M. Pavan, M. Neeb, A. K. Schaper, A. Danani, G. Klebe, O. M. Merkel, T. Kissel, *ACS Nano* **2012**, *6*, 9447.
[54] G. Gowrishankar, S. Zitzmann-Kolbe, A. Junutula, R. Reeves, J. Levi, A. Srinivasan, K. Bruus-Jensen, J. Cyr, L. Dinkelborg, S. S. Gambhir, *PLoS One* **2011**, *6*, e26902.
[55] I. Hamann, D. Krys, D. Glubrecht, V. Bouvet, A. Marshall, L. Vos, J. R. Mackey, M. Wuest, F. Wuest, *FASEB J.* **2018**, *32*, 5104.
[56] P. Dosta, V. Ramos, S. Borrós, *Mol. Syst. Des. Eng.* **2018**, *3*, 677.
[57] N. Nahrjou, A. Ghosh, M. Tanasova, *Int. J. Mol. Sci.* **2021**, *22*, 5073.


© 2023 The Authors. Macromolecular Bioscience published by Wiley-VCH GmbH